

# Analysis of Photon Scattering Trends for Material Classification using Artificial Neural Network Models

M. Iqbal Saripan<sup>1\*</sup>, Member IEEE, Wira Hidayat Mohd Saad, Student Member IEEE, Suhairul Hashim, Member IEEE, Ahmad Taufek Abdul Rahman<sup>3</sup>, Member IEEE, Kevin Wells<sup>4</sup> and David Andrew Bradley<sup>4</sup>

**Abstract**— In this project, we concentrate on using the Artificial Neural Network (ANN) approach to analyze the photon scattering trend given by specific materials. The aim of this project is to fully utilize the scatter components of an interrogating gamma-ray radiation beam in order to determine the types of material embedded in sand and later to determine the depth of the material. This is useful in a situation in which the operator has no knowledge of potentially hidden materials. In this paper, the materials that we used were stainless steel, wood and stone. These moderately high density materials are chosen because they have strong scattering components, and provide a good starting point to design our ANN model. Data were acquired using the Monte Carlo N-Particle Code, MCNP5. The source was a collimated pencil-beam projection of 1 MeV energy gamma rays and the beam was projected towards a slab of unknown material that was buried in sand. The scattered photons were collected using a planar surface detector located directly above the sample. In order to execute the ANN model, several feature points were extracted from the frequency domain of the collected signals. For material classification work, the best result was obtained for stone with 86.6% accurate classification while the most accurate buried distance is given by stone and wood, with a mean absolute error of 0.05.

**Index Terms**—Material classification, depth determination, stainless steel, wood, MCNP, Artificial Neural Network.

Accepted at: IEEE Trans Nuc Sci Jan 2013  
M.I. Saripan et al., IEEE Trans Nuc Sci (2013) 60, 2, 515 - 519  
doi: [10.1109/TNS.2012.2227800](https://doi.org/10.1109/TNS.2012.2227800)  
<http://ieeexplore.ieee.org/xpl/articleDetails.jsp?arnumber=6412756>

Manuscript received May 14, 2012. This work was supported by Ministry of Higher Education (ERGS)

<sup>1</sup>M.I.Saripan and W.H. Mohd Saad are with FRG Biomedical Engineering, Universiti Putra Malaysia, 43400 Serdang, Selangor, MALAYSIA (e-mail: iqbal@eng.upm.edu.my)

<sup>2</sup>S.Hashim is with the Department of Physics, Universiti Teknologi Malaysia, 81310 Skudai, Johor, MALAYSIA (phone: +607-5534195; fax: +607-5566162; e-mail: suhairul@utm.my).

<sup>3</sup>A.T.A.Rahman is with the School of Physics and Material Studies, Faculty of Applied Sciences, Universiti Teknologi MARA Malaysia, Campus of Negeri Sembilan, 72000 Kuala Pilah, Negeri Sembilan, MALAYSIA (e-mail: ahmadtaufek@ns.uitm.edu.my).

<sup>4</sup>K.Wells and D.A.Bradley is with Department of Physics, University of Surrey, Guildford, GU2 7XH, U.K (e-mail: k.wells@surrey.ac.uk and d.a.bradley@surrey.ac.uk)

## I. INTRODUCTION

Recent studies have shown that the pattern of scattered photons collected following the interaction of high energy gamma rays with absorbing media could be useful in determining unknown buried material [1-3]. In particular, this concerns photon-induced positron annihilation radiation (PIPAR), applied to issues of security [4]. In current implementation, the classification of the material relies on the raw signals collected from a scintillator detector [5].

To overcome limitations arising from use of a scintillator detector, Bradley et al. [6] demonstrated that the raw signals collected from the scintillator can be fully utilized by introducing an intelligent system to assist the decision making. In that work, use was made of a template matching system based on the sum of absolute differences (SAD) to calculate the best match to a particular material. Although the work yielded highly accurate results, accuracy is dependent to large extent on the similarity index between the template and the unknown incoming signals. Moreover, since the templates are based on energy spectra in the real domain, slight differences in terms of the response of the detector will affect the similarities between the template and the incoming signal.

This paper aims to extend the work in [6] by implementing a more complicated artificial intelligence method that does not depend on real domain similarities. In addition to the material classification, this paper also explores the use of this method to determine the buried depth of a given material in sand.

In the next section, a flowchart of the work is presented together with the simulation set-up. This is followed by results and discussion, including factors that can be used to support the conclusions.

## II. MATERIALS AND METHODS

### A. Overall methodology

Fig. 1 shows a flowchart of the main activities in this work. We started the work by gathering a real/time domain energy spectrum based on a fixed set-up as shown in the next section. The simulation set-up was constructed using Monte Carlo N-Particle Code MCNP5 [7] based on the same model as in [6]. Next, the collected raw signals have been processed in order to extract suitable features that could be useful in optimizing the ANN model. There were two sets of ANN in our work:

ANN1 is used to classify the type of materials hidden in sand, and ANN2 is used to determine the buried depth in sand. These two ANNs work in a sequential mode, with ANN2 dependent on the results given by ANN1.

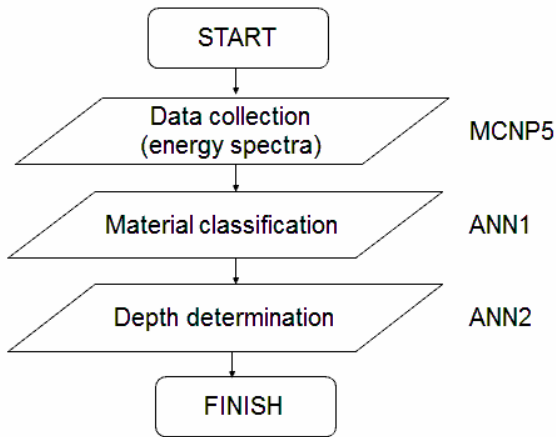


Fig. 1. Flowchart of the work on material classification and depth of the buried material

### B. Data Acquisition

The data were collected from a simulated experimental set-up that was constructed using the Monte Carlo N-Particle Code MCNP5. A 1 MeV gamma ray point source was used to represent a collimated pencil-beam projection, projected directly towards the surface of the slab of buried media. The material of this slab is interchangeable between stainless steel, stone and wood. The compositions of the materials are shown in Table 1.

Table 1: The list of materials used in this work

Material	Density (g/cm <sup>3</sup> )	Element	Fractional Composition (Mass)
Stainless steel	8.0	C	0.000400
		Si	0.005000
		P	0.000230
		S	0.000150
		Cr	0.190000
		Mn	0.010000
		Fe	0.701730
		Ni	0.092500
Stones	2.662	H	0.001657
		C	0.026906
		O	0.488149
		Na	0.012403
		Mg	0.023146
		Al	0.054264
		Si	0.246249
		S	0.000577
		K	0.018147

		Ca	0.089863
		Ti	0.003621
		Mn	0.000386
		Fe	0.033377
		Pb	0.001255
Wood	0.64	H	0.059642
		C	0.497018
		N	0.004970
		O	0.427435
		Mg	0.001988
		S	0.004970
		K	0.001988
		Ca	0.001988

Fig. 2 shows the geometrical graphic of the set-up. The detector was placed directly on top of the slab to capture the photons due to scattering and annihilation process. In order to study the pattern of the raw scattered photons, we omit the thickness of the detector and instead, just use an infinitely thin surface to count the number of photons scattered and which travel within the acceptable angle. MCNP5 will generate an output listing file of the photons that travel through the surface and in so doing, the energy spectra can be plotted without the effect of the scattering in the detector. Although all the dimensions are given in Fig. 2, none of them are treated as features or inputs, and ANN2 is used to estimate the depth of the buried target from the surface. The details of the features used in ANN1 and ANN2 are explained in the next section.

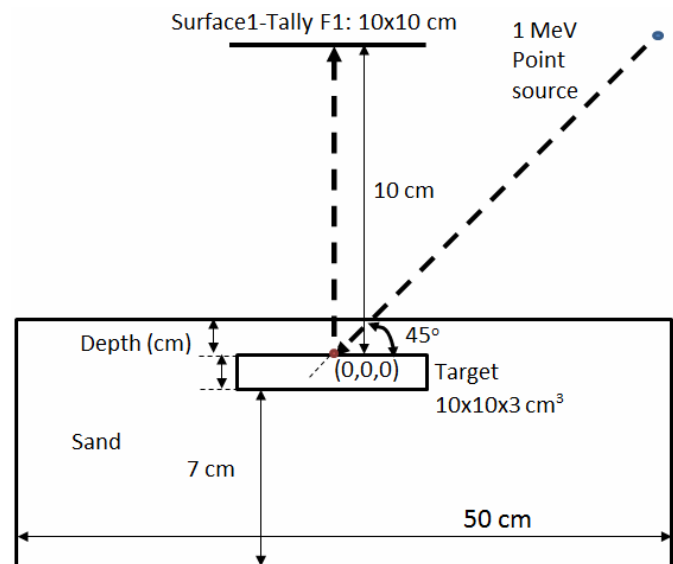


Fig. 2. The geometrical set-up of the MCNP5 simulation

Fig. 3 shows the photons tracking view in a visual editor of MCNP, known as MCNPVised. MCNPVised is used to create the geometry according to the dimensions given in Fig. 2 and to check the accuracy of the geometrical set up.

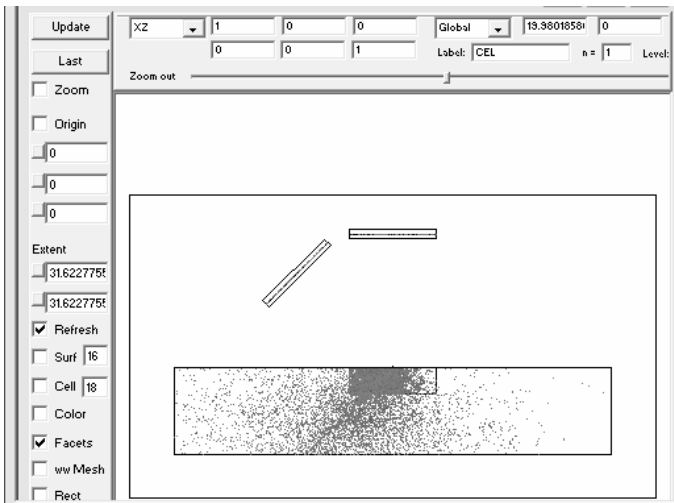


Fig. 3. The fate of incident photons tracked in MCNPVised

### C. Artificial Neural Network (ANN) and Features Extraction

The construction of ANN requires specific features to be extracted as patterns or trends that will be ‘remembered’ by the neurons. In order to distinguish between materials or distances, the selected features must be able to provide unique patterns that can immediately be correlated with the type of materials, or the buried depths in sand. Initially, ANN will be trained during the training stage by providing the known material and depths as the output of the training. Once both ANN1 and ANN2 have been trained to remember the patterns or trends, the data gathered from MCNP simulation are used in the testing stage.

In this paper, we propose the use of trends in the frequency domain of the energy spectra. The steps taken to obtain the features can be summarized as follows: (1) raw energy spectra are transformed to their frequency components using Discrete Fourier Transform (DFT), (2) the magnitude of the frequency spectra are normalized by the total magnitude value, (3) frequency points from direct current (DC) value to the highest frequency point are recorded in fifty individual steps. These points are used as the features in our proposed ANN model.

## III. RESULTS AND DISCUSSION

### A. Features

As described in the previous section, the features used in our ANN model were extracted from the frequency spectra of the energy spectra. Fig. 4 shows the energy spectra gathered for stainless steel, stone and wood. As shown in the figure, the obvious difference between the materials can be extracted from a few regions. However, as the material is buried progressively deeper in sand, the scattered photons will easily amplify the scattering regions of the plot. To overcome the problem, the features are extracted from the frequency domain of the signals.

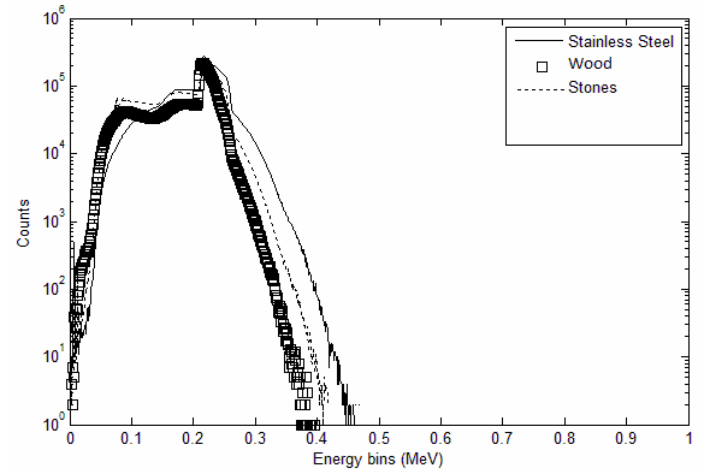


Fig. 4. Energy spectra for stainless steel, wood and stone.

Fig. 5. shows the frequency spectra of the original recorded energy spectra for stainless steel, wood and stone. Even though the differences are quite small in the low frequency region, as the frequency increases a greater difference can be observed. Comparing the frequency spectra to the original energy spectra, the former is more robust than the latter because the magnitude in frequency domain is not affected by different number of counts in the adjacent bins.

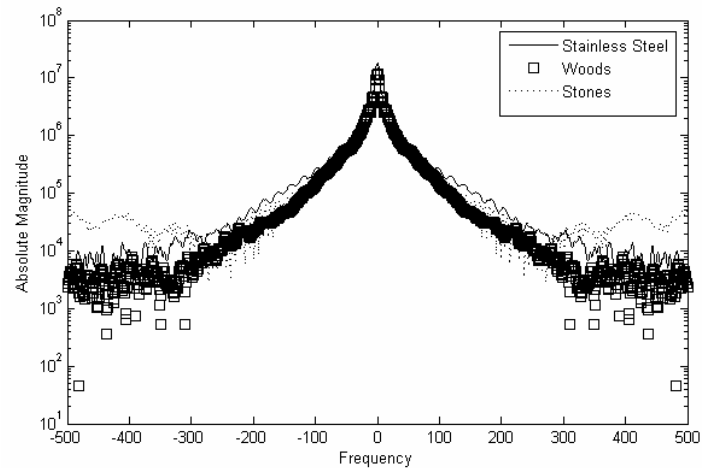


Fig. 5. Frequency spectra of stainless steel, wood and stone.

### B. ANN1 Model for Material Classification

Once the energy spectra have been transformed to their frequency spectra, we extracted the four points from the high frequency region. Different seeds were simulated to model different signals collection. Fig. 6 shows the structure of ANN1 that we used to classify the material.

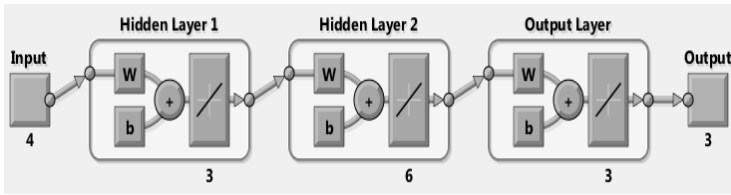


Fig. 6. The feedforward backpropagation structure of ANN1 for material classification.  $w$  is weight and  $b$  is bias.

The structure that we used is based on four inputs extracted from four high frequency points from each material. Then, we have used two hidden layers where the first layer has three neurons and the second one has six neurons. The outputs are three values that have been trained to follow this matrix:

$$\text{ANN1 Output} = \begin{bmatrix} 1 & 0 & 0 \\ 0 & 1 & 0 \\ 0 & 0 & 1 \end{bmatrix} \quad (1)$$

where (1,0,0) output given from the above equation refers to stainless steel, (0,1,0) refers to stone and (0,0,1) refers to wood.

The results for all three materials are as follows: stainless steel yielded 86.6% accuracy, stone yielded 95.1% and wood recorded the lowest accuracy of 48.6%. Once the materials have been classified, ANN2 is used to determine the depth distance of the slab buried in sand.

*C. ANN2 Model for Depth Distance Determination*

Instead of using the high frequency regions, ANN2 used five low frequency points as its features. Fig. 7, 8 and 9 show the low frequency regions for stainless steel, stone and wood, respectively. Although the plots are quite close to one another, since we used five points, therefore instead of remembering as points, ANN will remember as patterns or trends.

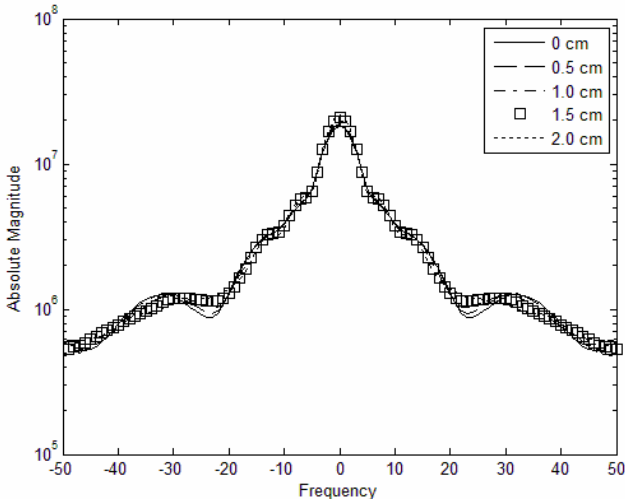


Fig. 7. Low frequency components of stainless steel

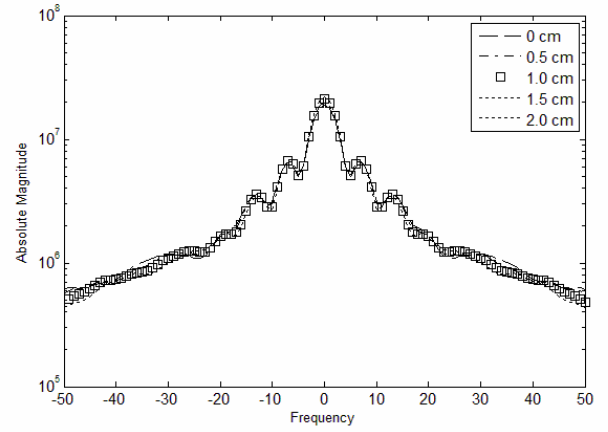


Fig. 8. Low frequency components of stone

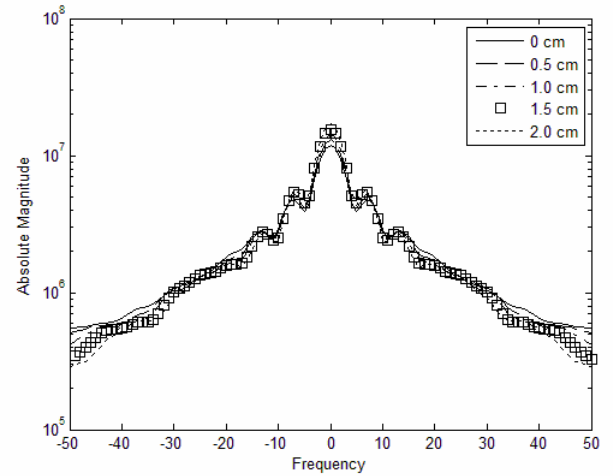


Fig. 9. Low frequency components of wood

Fig. 10 shows the ANN2 model that consists of five inputs, one hidden layer with five neurons and one output. The inputs for this model are the low frequency components of each samples and the output is the estimated distance of the samples from the surface.

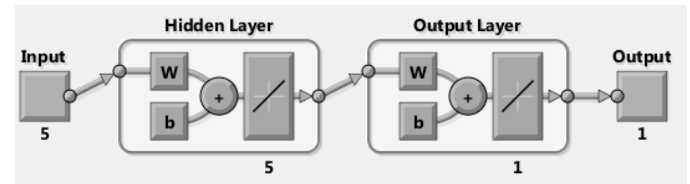


Fig. 10. The feedforward backpropagation model used by ANN2

Unlike the output that was arranged in a form of a matrix in ANN1 model, ANN2 used a single line output to record the distance in  $cm$ , as follows:

$$\text{ANN2 Output} = [0.0 \ 0.5 \ 1.0 \ 1.5 \ 2.0] \quad (2)$$

The results given for all three materials are given in Table 2 to 4. The data shown in the first rows of Table 2 to 4 are the original data set in the simulation and the second rows are the estimated depth given by ANN2. After that, the mean absolute

error (MAE) is calculated by taking the error values at each depths and calculate the absolute average errors. The step can be shown in the following equation:

$$MAE = \frac{|(\text{original}-\text{obtained})|}{5} \quad (3)$$

Table 2: Results for stainless steel

Original	0.0cm	0.5cm	1.0cm	1.5cm	2.0cm
Obtained	0.01cm	0.46cm	1.05cm	1.54cm	2.27cm
MAE	0.09				

Table 3: Results for stone

Original	0.0cm	0.5cm	1.0cm	1.5cm	2.0cm
Obtained	0.20cm	0.53cm	1.02cm	1.51cm	2.01cm
MAE	0.05				

Table 4: Results for wood

Original	0.0cm	0.5cm	1.0cm	1.5cm	2.0cm
Obtained	0.06cm	0.56cm	1.09cm	1.51cm	2.00cm
MAE	0.05				

The results given in Table 2 to 4 indicated small errors given by the ANN2 model for all three types of material. This is a very interesting finding in demonstrating the successful use of ANN in this work.

#### IV. CONCLUSIONS

This paper has demonstrated the use of Artificial Neural Network (ANN) not only to classify different materials, but also to determine the buried depth of the unknown material in sand. The results show stone to produce the best classification result, also recording the lowest error in buried depth determination, together with wood. Therefore, we can conclude that frequency spectra are useful and adequate to be used as features in ANN.

More work is currently being conducted in an effort to more closely define features that increase the overall accuracy of the system. The structure or model of ANN can also be improved by investigating the optimum number of hidden layers and the type of neural network.

#### ACKNOWLEDGMENT

M. I. Sariipan would like to acknowledge Ministry of Higher Education Malaysia under ERGS research grant scheme ERGS/1/11/TK/UPM/02/24 vot number 5527023.

#### REFERENCES

- [1] J.D.Lowrey, W.L.Dunn, Signature-based radiation scanning using radiation interrogation to detect explosives., Applied Radiation Isotopes Vol 68, pp893-895, 2010.
- [2] W.L.Dunn, R.Brewer, K.W.Loschke, and J.D.Lowrey, Radiation interrogation using Signature Analysis for detection of chemical explosives, in: Proceedings of the IEEE Conference on Technologies for Homeland Security: Enhancing Critical Infrastructure Dependability, pp.7-12, 2007
- [3] W.L.Dunn, C.J.Solomon, K.W.Loschke, D.A.Bradley and W.B.Gilboy, Ionizing photon methods for standoff bomb detection, Nuclear Instruments and Methods in Physics Research A, Vol 580, pp778-781, 2007.
- [4] G.Harding, W.Gilboy, B.Ulmer, Photon-induced positron annihilation radiation (PIPAR) — A novel gamma-ray imaging technique for radiographically dense materials, Nuclear Instruments and Methods in Physics Research A, Vol 398, pp409-422, 1997.
- [5] R.L. Brewer, W.L. Dunn, S. Heider, C. Matthew, X. Yang, The signature-based radiation-scanning approach to standoff detection of improvised explosive devices, Applied Radiation and Isotopes, Vol 70(7), pp1181-1185, 2012
- [6] D.A. Bradley, S.Hashim, M.I.Saripan, K.Wells, W.L.Dunn, Nuclear Instruments and Methods in Physics Research A, Vol 652, pp466-469, 2011
- [7] X-5 Monte Carlo Team—A General Monte Carlo N-Particle Transport Code, MCNP, Version5, Los Alamos National Laboratory, 2008.